41st AIAA/ASME/SAE/ASEE Joint Propulsion Conference & Exhibit
10 - 13 July 2005, Tucson, Arizona

AIAA 2005-3549

41th AIAA/ASME/ASEE Joint Propulsion Conference, Tucson, Az, July 2005. AIAA 2005-3549

Check for updates

Modeling of Propellant Tank Pressurization

Greg Zilliac*
NASA Ames Research Center, Moffet Field, Mountain View, CA 94035

And

M. Arif Karabeyoglu†
Stanford University, Stanford, CA 94305

Accurate modeling of propellant tank pressurization is an essential element of the prediction of rocket performance. This is the case even more so for hybrid rockets that use a self-pressurizing oxidizer because the thrust produced by the motor is dependent on oxidizer tank pressure. Described herein is a real fluid, quasi-phase equilibrium thermodynamic propellant tank model that is applicable to a broad range of propellants including those that are highly volatile and/or cryogenic. The model has been validated by comparison with the measured results of cold-flow blow-down tests of a self-pressurizing nitrous oxide system. Data from one of the cold-flow tests showed evidence of stratification within the oxidizer tank during the blow down. It was found that accurate modeling of the propellant evaporation rate is a crucial element in the prediction of the propellant expulsion process.

Downloaded by STANFORD UNIVERSITY on April 12, 2022 | http://arc.aiaa.org | DOI: 10.2514/6.2005-3549

Nomenclature

A	= area
a	= acceleration or equation-of-state term
b	= equation of state term
C	= Nusselt number coefficient
C_D	= discharge coefficient
c_p	= specific heat capacity at const. pressure
c_v	= specific heat at constant volume
D	= cylindrical tank diameter
E	= evaporation coefficient or total energy
F	= function of Z and T_r
f	= friction factor
G	= mass velocity
h	= specific enthalpy or heat transfer coeff.
K	= bulk modulus
k	= thermal conductivity
L	= length
M	= molecular weight
m	= mass
n	= Nusselt number exponent
P	= pressure
$\dot{Q}$	= heat transfer rate
R_e	= Reynolds number
R_u	= universal gas constant
T	= temperature
t	= time
U	= internal energy
u	= specific internal energy
$\tilde{u}$	= velocity
v	= specific volume
V	= volume
W	= work
X	= Grashof -Prandtl number product
Y	= weight fraction or expansion factor
y	= mole fraction
z	= liquid level
Z	= compressibility factor
a	= Peng-Robinson eq. of state function
b	= thermal coeff. of volumetric expansion
Δ	= difference
k	= function of ω
m	= absolute viscosity
r	= density
w	= acentricity factor

Subscripts and Superscripts

A	= air
B	= component b (evaporation or boiling)

* Research Scientist, NASA Ames Research Center/M.S. 260-1, Member AIAA.
† Research Associate, Dept. of Aeronautics and Astronautics, Stanford University, Member AIAA.

This material is declared a work of the U.S. Government and is not subject to copyright protection in the United States.

c	= critical or combustion chamber
C	= condensation
F	= film
G	= gas
ig	= ideal gas
L	= liquid
lv	= latent heat of vaporization
m	= molar
$prop$	= propellant
R	= reference condition
r	= reduced
S	= surface
SAT	= saturation
T	= tank
U	= lower extreme of surface layer
V	= vapor
W	= wall

Combined Subscripts

AR	= air recovery (temperature)
AWG	= exterior wall adjacent to ullage
AWL	= exterior wall adjacent to liquid
GS	= gas surface
GSF	= gas surface film
GW	= interior ullage wall
GWF	= gas wall film
LS	= liquid surface layer
PG	= pressurant gas
$PROP$	= propellant
TG	= tank (or ullage) vapor-gas mixture
VL	= vaporized liquid
VLB	= evaporated (or boiled) liquid
VLC	= condensed vapor
VLS	= vapor liquid surface
SA	= exterior surface air
WL	= wall liquid

I. Introduction

For chemical propulsion systems that rely on the volatility of the oxidizer to generate ullage pressure (i.e. a self-pressurizing propellant system), accurate knowledge of the expected ullage pressure is essential to accurately predict the performance of the rocket. For instance, the initial thrust of a simple N_2O/hydro-carbon hybrid rocket system is predicted to be 28% less on a cold day than on a hot day. The reason for this is that the ullage pressure in the N_2O propellant tank is 6.2 Mpa at 303 K, but only reaches 3.3 Mpa at 275 K. Furthermore, as oxidizer is removed from a propellant tank, the ullage pressure decreases, but the phase change from liquid to gas within the tank results in a substantial increase in ullage pressure above that predicted if evaporation is ignored (typically for N_2O, up to 35%, with a corresponding, but smaller, impact on the thrust).

Most propellants have the ability to self-pressurize to a degree and self-pressurization is often the best option for small to moderate sized rockets yet, in recent years, little attention has been placed on the modeling of pressurization systems that is directly relevant to boosters or sounding rockets (i.e. with the inclusion of propellant expulsion, and vehicle acceleration).

One of the most comprehensive treatments of rocket pressurization systems is that presented by Ring[1] in the compendium entitled "Rocket Propellant and Pressurization Systems". In particular, the thermodynamic model described by Traxler and Kenny, in this reference, has been the starting point for many pressurization system modeling efforts described in the open literature since (as is the case for the current effort). The chief difficulty with the Traxler and Kenny model is the assumption of ideal fluid behavior. In addition, the rate of propellant vaporization (and also condensation) is modeled in a rudimentary manner leading to an inaccurate prediction of ullage pressure for highly volatile propellants.

Pasley[2] developed a mathematical model of the pressure-fed propellant tank used on the Lunar Surveyor. The quasi-equilibrium thermodynamic model compared well with ground and flight test measurements of the pressurant tank pressure. The main conclusion of this study was the importance of correctly modeling the heat transfer between the pressurant gas and the propellant tank wall. It was found that the total pressurant system mass prediction could vary by up to eight percent depending on the level of approximation used to model the heat transfer.

In reference 3, a complete cryogenic pressurization system for a pump-fed motor, including the system response during cool-down and pump priming prior to motor firing, and the response during motor firing, was

Downloaded by STANFORD UNIVERSITY on April 12, 2022 | http://arc.aiaa.org | DOI: 10.2514/6.2005-3549

modeled. The predicted ullage pressure time history compared well with that measured during a firing even though the ullage temperature predictions differed significantly from those measured (by 28 K on average). The explanation for the ullage temperature discrepancy, given by the authors, was that stratification effects, present in the ullage gas, were not measured by the single-point ullage-gas temperature measurement. This conclusion seems at odds with the generally held belief that the ullage gas is stirred by natural convection and therefore should be relatively uniform in temperature.

A finite-volume approach to the modeling of a pressure-fed system was developed by Majumdar et al.[4] Although no actual measured data were used for validation, a sensitivity analysis showed that the ullage temperature was very sensitive to the heat transfer coefficient used to model the heat transfer from the ullage gas-vapor mixture to the liquid propellant. They found that this heat transfer rate directly affects the rate of propellant vaporization.

A sophisticated cryogenic propellant tank model that used a finite element method applied to the Navier-Stokes equations to model the liquid and a lumped thermodynamic model of the vapor region was developed in reference 5. Various approaches to heating and stirring were studied. It was found that the propellant tank pressure was greatly impacted by heat addition to the vapor. Furthermore, the finite element results showed that the temperature distribution in the undisturbed liquid can become stratified under various heat addition scenarios unless the liquid is stirred.

In reference 6, a highly analytical approach was taken to the validity of lumped thermodynamic models and their ability to predict phase change – the essential characteristic of propellant tank modeling. It was shown that the perfect gas and perfect liquid assumptions are inadequate and that higher order equations of state (i.e. van der Waals or similar) are required in order to predict evaporation and condensation.

One can surmise from the previous modeling efforts that accurately predicting the heat and mass transfer across the liquid-vapor interface is essential but also problematic. It is also evident that the development of a pressurization system model that is applicable to all situations is difficult to achieve. The main obstacle is that assumptions have to be made concerning the heat transfer mechanisms (i.e. conduction, free or forced convection). Often, the type of heat transfer changes during the pressurization process.

For instance, in the N_2O self-pressurizing system typically employed in small sounding rockets, the temperature throughout the system is equal to the ambient temperature and no significant heat transfer takes place just prior to the start of a blow down. The vapor and liquid are in phase equilibrium. As soon as the valve is opened and liquid begins to flow from the tank, the temperature of the ullage vapor starts to decrease (through expansion). The ensuing temperature differences between the tank walls, the liquid surface and the vapor in the ullage results in heat transfer by natural convection in the ullage. Convection is also initiated within the liquid. The reduction of the temperature of the ullage vapor is accompanied by a reduction in the vapor pressure leading to evaporation of liquid that continues until phase equilibrium is restored. Typically, liquid is removed from the tank at a high enough rate that the pressure in the ullage continuously decreases but the evaporation rate, for many propellants, is high enough to significantly reduce the pressure reduction resulting from expansion.

Under certain circumstances, a relatively simple model of the mass transfer between the liquid and vapor phases in a propellant tank can be constructed by assuming that the vapor in the ullage is always saturated when liquid is present in the tank. Conservation equations are applied to the system as a whole and the liquid fraction is determined along with the ullage pressure without explicit consideration of the heat and mass transport occurring between the liquid and vapor phases. The main assumption is that the temperature is uniform throughout the tank and equal to the saturated-liquid temperature at any point in time. This approach works well when the liquid expulsion rate is low. At moderate to high propellant mass flow rates, the bulk liquid does not have time to achieve a uniform temperature and therefore, more sophisticated modeling that explicitly includes the heat and mass transfer rate across the liquid-vapor interface is required.

In the following sections, a propellant tank model is described, followed by a comparison with the results of several blow-down tests. The model does not assume phase equilibrium and is applicable to

Downloaded by STANFORD UNIVERSITY on April 12, 2022 | http://arc.aiaa.org | DOI: 10.2514/6.2005-3549

propellants that exhibit real fluid behavior. A crucial aspect of the overall model is the method used to predict propellant evaporation which is discussed in Appendix A.

II. Modeling Approach

The main goal in the current modeling effort is to develop a model of a propellant feed system that can be readily incorporated into a rocket design computer program. The model developed is general and should work well for propellant tanks that are pressure fed with an inert gas and also for self-pressurizing systems. In self-pressurizing systems, the liquid in the propellant tank is volatile and typically no inert gas is introduced. Pressure in the ullage is generated through a propellant vaporization process. During propellant utilization, the liquid flow out of the tank is usually followed by a vapor flow that can be used to produce thrust. This vapor portion (or gas-vapor mixture when a pressurant is used) of the flow is also modeled.

To maintain generality, self-pressurizing systems are treated in the same manner as pressure-fed systems even though they are fundamentally different from a thermodynamic point of view. For instance, in self-pressurizing systems, only two phases of the same substance are present. The main implication is that, if the system is considered to be in phase equilibrium, the temperature at the vapor-liquid interface is that corresponding to the saturated vapor pressure. Accordingly, Gibbs' phase rule dictates that the thermodynamic properties are a function of only one intensive variable and the rate of mass transfer between the vapor and liquid is governed by diffusion. In simple pressure-fed systems, a minimum of two phases and two components are present. Knowledge of at least two intensive variables is required to define a property (with the partial pressure typically being one of the intensive variables). Convective heat transfer is possible as is boiling.

In reality, a self-pressurized system is not in phase equilibrium because it is an open system with irreversible heat and mass transfer. In such systems, a temperature jump can be sustained across the vapor-liquid interface. The possible existence of a vapor-liquid interfacial temperature jump alters the primary boundary condition that establishes the propellant evaporation rate and hence the ullage pressure. Even so, for many propellant systems, the interfacial temperature jump is thought to be small. Therefore, in the current modeling effort, the temperature at the liquid-vapor interface is assumed to be the vapor saturation temperature.

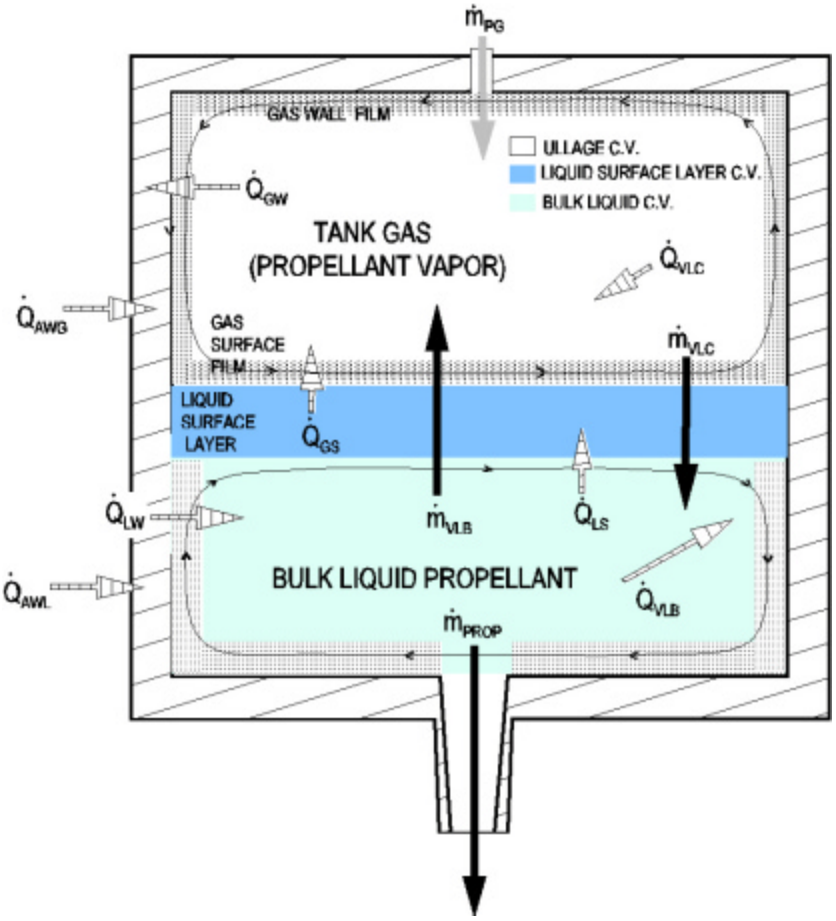

Figure 1. Schematic of the propellant tank model.

Downloaded by STANFORD UNIVERSITY on April 12, 2022 | http://arc.aiaa.org | DOI: 10.2514/6.2005-3549

A complete description of the model would be difficult to present within the space limitations of this paper. The reader is referred to reference 1 for supplementary information concerning thermodynamic modeling of propellant tanks (for consistency, the same notation has been used).

As seen in Fig. 1, the model consists of three regions, namely, the bulk liquid, the liquid surface layer and the bulk gas in the ullage that can contain vapor and also inert and residual gases. Arrows indicate the predominant heat and mass transfer directions and the subscripts indicate the phase of the quantity being transferred and also some information about the origin and destination of the transferred quantity (see Table 1).

It is assumed that the temperature and composition of the bulk liquid and also of the gas are uniform. Temperature varies across the thin liquid surface layer but is spatially constant within the ullage gas and the bulk liquid.

The necessity of defining a thin liquid surface layer arises from the observation that temperature gradients, associated with convective heat transfer, are large near surfaces (i.e. a thermal boundary layer exists). In the lumped approach to modeling used here, the continuous temperature variation within the tank is modeled with the bulk liquid at a temperature of T_L, the liquid surface is at T_S, and the ullage vapor (or gas) is at T_{TG}.

Table 1. Transferred quantities

Quantity	Description
$\dot{Q}_{GW}$	Heat transferred between the tank wall and the ullage gas by convection of the ullage gas.
$\dot{Q}_{GS}$	Heat transferred between the ullage gas and the liquid surface layer by convection of the ullage gas.
$\dot{Q}_{VLC}$	Heat added to the ullage gas through condensation (if any).
$\dot{Q}_{VLB}$	Heat removed from the bulk liquid to produce a phase change from liquid to a vapor
$\dot{Q}_{LW}$	Heat transferred between the tank wall and the bulk liquid by convection of the bulk liquid.
$\dot{Q}_{LS}$	Heat transferred between the bulk liquid and the liquid surface layer through convection of the bulk liquid.
$\dot{Q}_{AWL}$	Heat transferred between the external environment and the tank wall adjacent to the bulk liquid.
$\dot{Q}_{AWG}$	Heat transferred between the external environment and the ullage wall.
$\dot{m}_{PG}$	Mass flow rate of the pressurant gas added to the tank (if any).
$\dot{m}_{VLB}$	Mass flow rate of propellant vaporization (i.e. evaporation, boiling…etc.)
$\dot{m}_{VLC}$	Mass flow rate of propellant condensation.
$\dot{m}_{PROP}$	Mass flow rate of the propellant being withdrawn from the tank.

Equations expressing the conservation of energy and mass are integrated in time to determine the bulk temperature, pressure and mass within the tank. The subscript "TG" is used to refer to the ullage gas that may consist of only propellant vapor or a spatially uniform mixture of pressurant gas and propellant vapor. If the ullage gas is a mixture, mixing rules, that relate properties of the pure components to that of the mixture, should be applied.

Although the model developed is applicable to pressure-fed and self-pressurizing systems (or hybrids thereof), the emphasis of the current paper is on self-pressurizing systems.

Downloaded by STANFORD UNIVERSITY on April 12, 2022 | http://arc.aiaa.org | DOI: 10.2514/6.2005-3549

Governing Equations

Conservation equations for three regions within the propellant tank (i.e. ullage gas, bulk liquid and the liquid surface layer) are developed independently but since the regions share boundaries, the conservation equations are coupled. The general form of conservation of energy for a control volume enclosing an unsteady open process, assuming that potential energy changes associated with the control volume and fluid streams are negligible, can be written as:

$$\dot{Q}_{NET} + \sum_i \dot{m}_i (h_i + \frac{1}{2}\tilde{u}_i^{\,2}) = \dot{W} + \sum_e \dot{m}_e (h_e + \frac{1}{2}\tilde{u}_e^{\,2}) + \frac{dE_{CV}}{dt} \tag{1}$$

Where $\dot{Q}_{NET}$ is the rate of net heat input, $\dot{W}$ is the rate of net work output and $\frac{dE_{CV}}{dt}$ is the rate of accumulation of total energy within the control volume. The subscripts *i* and *e* refer to the control volume inlets and exits, respectively. For a control volume enclosing the ullage gas shown in Fig. 1, boundary work is performed because the system changes size with time (i.e. the control volumes associated with the ullage gas and the bulk liquid change size with time). Assuming that the energy is uniform along the inflow and outflow boundaries, the ullage gas control volume energy equation terms are:

$$\dot{Q}_{NET} = \dot{Q}_{GS} - \dot{Q}_{GW} + \dot{Q}_{VLC} \tag{2}$$

$$\sum_i \dot{m}_i h_i = \dot{m}_{PG} h_{PG} + \dot{m}_{VLB} h_{VLB} \tag{3}$$

$$\dot{W} = \frac{d}{dt}(PV) = P_{TG}\dot{V}_{TG} + \dot{P}_{TG} V_{TG} \tag{4}$$

$$\sum_e \dot{m}_e h_e = \dot{m}_{VLC} h_{LC} \tag{5}$$

$$\frac{dE_{CV}}{dt} = \frac{dU}{dt} = \frac{d}{dt}(m_{TG} u_{TG}) \tag{6}$$

The total specific enthalpy h and internal energy u are intensive properties of unknown absolute value. Because intensive properties are independent of the path that the system takes, h and u can be expressed as a sum of increments from a reference state. It is convenient to use departure functions, (e.g. $(h - h^{ig})_{T,P}$) to express the real gas and liquid enthalpy and internal energy relative to their "ideal gas reference state" values. The rationale for the use of departure functions will be discussed shortly. When using an ideal gas reference state, the propellant should behave as an ideal gas (i.e. $Z \cong 1.0$) at the reference temperature and pressure. For N_2O, the reference conditions selected are $T_R = 298.15$ K and $P_R = 1$ atm, for which, $Z = 0.9941$. The specific enthalpy and internal energy can be written as:

$$h_{T,P} = (h - h^{ig})_{T,P} + \int_{T_R}^{T} c_p{}^{ig}\, dT + h^{ig}{}_R \tag{7}$$

Downloaded by STANFORD UNIVERSITY on April 12, 2022 | http://arc.aiaa.org | DOI: 10.2514/6.2005-3549

$$u_{T,P} = (u - u^{ig})_{T,P} + \int_{T_R}^{T} c_v^{\,ig}\, dT + u^{ig}{}_R \tag{8}$$

The parenthetical terms above are the departure functions of the real fluid h and u properties from those of the ideal gas properties at the same temperature and pressure. The reference ideal gas internal energy $u^{ig}{}_R$ can be arbitrarily set to zero. Since for an ideal gas, $h^{ig} = u^{ig} + Pv$ and $Pv = R_u T / M$, therefore, $h^{ig}{}_R = R_u T_R / M$. In addition, $c_V^{\,ig} = c_P^{\,ig} - R_u / M$ and $c_P^{\,ig}$ can be expressed as a polynomial involving T that can be easily integrated (see Table 2). The above definition of internal energy can be substituted for u_{TG} in the energy accumulation term. This involves taking a time derivative. It can be shown that $\frac{d(u - u^{ig})_{T,P}}{dt} = F_1 \dot{T} + F_2 \dot{r}$ where F_1 and F_2 are functions of T, r and other quantities related to the fluid as expressed in the Thermodynamic Properties section of this paper. One can also show that $\frac{d}{dt}\int_{T_R}^{T} c_v^{\,ig}\, dT = c_v^{\,ig}\Big|_T \dot{T}$. Hence, the ullage energy accumulation term can be written as:

$$\frac{d}{dt}(m_{TG} u_{TG}) = \dot{m}_{TG} u_{TG} + m_{TG}\left(F_{1_{TG}} + c_{V_{TG}}{}_T^{\,ig}\right)\dot{T}_{TG} + m_{TG} F_{2_{TG}} \dot{r}_{TG} \tag{9}$$

When substituting in numerical values for enthalpy or internal energy, because of the approximations made above and the fact that for unsteady open systems, the reference state temperature often appears either implicitly or explicitly in the energy equation, it is important to use correct reference values. It should be noted that the use of an ideal gas reference state for a real fluid does not imply that the fluid is, in any way, ideal – it is simply a useful reference. For the ullage gas (when liquid is present in the tank), the kinetic energy terms are small in comparison to the enthalpy so they have been neglected. Conservation of energy for the ullage gas can then be written as:

$$\begin{aligned}&(\dot{Q}_{GS} - \dot{Q}_{GW} + \dot{Q}_{VLC}) + \dot{m}_{PG} h_{PG} + \dot{m}_{VLB} h_{VLB} - \dot{m}_{VLC} h_{LC} \\ &= (P_{TG}\dot{V}_{TG} + \dot{P}_{TG} V_{TG}) + \dot{m}_{TG} u_{TG} + m_{TG}\left(F_{1_{TG}} + c_{V_{TG}}{}^{ig}\right)\dot{T}_{TG} + m_{TG} F_{2_{TG}} \dot{r}_{TG}\end{aligned} \tag{10}$$

Solving for $\dot{T}_{TG}$:

$$\dot{T}_{TG} = \frac{\left(\dot{Q}_{GS} - \dot{Q}_{GW} + \dot{Q}_{VLC}\right) + \dot{m}_{PG} h_{PG} + \dot{m}_{VLB} h_{VLB} - \dot{m}_{VLC} h_{LC} - \left(P_{TG}\dot{V}_{TG} + \dot{P}_{TG} V_{TG}\right) - \dot{m}_{TG} u_{TG} - m_{TG} F_{2_{TG}} \dot{r}_{TG}}{m_{TG}\left(F_{1_{TG}} + c_{V_{TG}}{}^{ig}\right)} \tag{11}$$

The enthalpy associated with condensation (if conditions for condensation are satisfied) is h_{LC}. It is assumed that condensation takes place within the control volume associated with the ullage gas and therefore the condensed liquid enthalpy h_{LC} is evaluated at T_{TG}. Conservation of mass is stated as:

$$\dot{m}_{TG} = \dot{m}_{VLB} - \dot{m}_{VLC} + \dot{m}_{PG} \tag{12}$$

Downloaded by STANFORD UNIVERSITY on April 12, 2022 | http://arc.aiaa.org | DOI: 10.2514/6.2005-3549

Downloaded by STANFORD UNIVERSITY on April 12, 2022 | http://arc.aiaa.org | DOI: 10.2514/6.2005-3549

When the liquid is completely exhausted from the tank, the thermodynamics of multiple phases are no longer of concern (i.e. mass and heat transfer no longer take place between the vapor and liquid phases of the propellant). The thermodynamic properties of the gas are significantly different from those of the near saturated vapor properties used up to this point. The control volume remains fixed in size and so $\dot{W} = 0$. In addition, $\dot{m}_{prop} = -\dot{m}_{TG}$ and using the definition of enthalpy, $h_{TG} - u_{TG} = \frac{P_{TG} V_{TG}}{m_{TG}}$. Therefore, the rate of change of the tank gas temperature simplifies to:

$$\dot{T}_{TG} = \frac{-\dot{Q}_{GW} + \dot{m}_{PG} h_{PG} - \dot{m}_{PROP}\left(\frac{P_{TG} V_{TG}}{m_{TG}} + \frac{1}{2}\tilde{u}_e^{\,2}\right) - m_{TG} F_{2_{TG}} \dot{r}_{TG}}{m_{TG}\left(F_{1_{TG}} + c_{V_{TG}}^{\,ig}\right)} \tag{13}$$

The above expression includes the term $\frac{1}{2}\tilde{u}_e^{\,2}$ that is associated with the kinetic energy of the gas leaving the control volume. This term is small in comparison to $\frac{P_{TG} V_{TG}}{m_{TG}}$ but in some cases it may not be negligible when the flow exiting the propellant tank is a vapor or gas only flow. In the unusual case of a propellant vapor that behaves as an ideal gas, if the heat transfer and kinetic energy effects are neglected and no pressurant gas is injected (i.e. $F_{1_{TG}}$, $F_{2_{TG}}$ $\dot{Q}_{GW}$, $\frac{1}{2}\tilde{u}_e^{\,2}$ and $\dot{m}_{PG}$ are set to zero), this differential equation has an exact solution of $\ln\left(\frac{T_f}{T_i}\right) = \frac{R_u}{M c_V}\ln\left(\frac{m_f}{m_i}\right)$ where i and f are the initial and final values, respectively. For a calorically perfect gas, this result simplifies to $\ln\left(\frac{T_f}{T_i}\right) = (g-1)\ln\left(\frac{m_f}{m_i}\right)$.

Conservation of energy applied to a control volume containing the bulk liquid leads to the following:

$$\dot{Q}_{NET} = \dot{Q}_{LW} - \dot{Q}_{LS} - \dot{Q}_{VLB} \tag{14}$$

$$\sum_i \dot{m}_i h_i = \dot{m}_{VLC} h_L \tag{15}$$

$$\dot{W} = \frac{d}{dt}(PV) = P_L \dot{V}_L + \dot{P}_L V_L \tag{16}$$

$$\sum_e \dot{m}_e h_e = \dot{m}_{VLB} h_{VLB} + \dot{m}_{PROP} h_L \tag{17}$$

$$\frac{dE_{CV}}{dt} = \frac{dU}{dt} = \frac{d}{dt}(mu) = \dot{m}_L u_L + m_L\left(F_{1_L} + c_{V_L}^{\,ig}\right)\dot{T}_L + m_L F_{2_L} \dot{r}_L \tag{18}$$

Hence:

$$\begin{aligned}&(\dot{Q}_{LW} - \dot{Q}_{LS} - \dot{Q}_{VLB}) + \dot{m}_{VLC} h_{LC} - \dot{m}_{PROP} h_L - \dot{m}_{VLB} h_{VLB} \\ &= (P_L \dot{V}_L + \dot{P}_L V_L) + \dot{m}_L u_L + r_L V_L \left(F_{1_L} + c_{V_L}{}^{ig}\right) \dot{T}_L + m_L F_{2_L} \dot{r}_L\end{aligned} \tag{19}$$

$$\dot{T}_L = \frac{(\dot{Q}_{LW} - \dot{Q}_{LS} - \dot{Q}_{VLB}) + \dot{m}_{VLC} h_{LC} - \dot{m}_{PROP} h_L - \dot{m}_{VLB} h_{VLB} - \left(P_L \dot{V}_L + \dot{P}_L V_L\right) - \dot{m}_L u_L - m_L F_{2_L} \dot{r}_L}{r_L V_L \left(F_{1_L} + c_{V_L}{}^{ig}\right)} \tag{20}$$

In the above energy conservation expression for the bulk liquid, $c_{V_L}{}^{ig}$ is present because the ideal gas reference state is used for the liquid as well as the vapor. Since the phase change from liquid to vapor is assumed to occur within the bulk liquid, the enthalpy associated with the vapor leaving the bulk liquid, h_{VLB} is the enthalpy of vapor evaluated at the bulk liquid temperature T_L. The term $m_L F_{2_L} \dot{r}_L$ in the above equation can cause some numerical instabilities during the integration process (i.e. care must be taken when numerically differentiating r_L with respect to time). Conservation of mass applied to the bulk liquid is stated as:

$$\dot{m}_L = \dot{m}_{VLC} - \dot{m}_{VLB} - \dot{m}_{PROP} \tag{21}$$

For many propellants, one cannot assume that the liquid is incompressible. For instance, the density of liquid N_2O increases by 17.8 percent while liquid is being expelled in the case 1 blow-down test (presented in the Model Validation part of the paper).

The conservation of mass and energy expressions can be numerically integrated in time to determine T_{TG}, T_L, m_{TG} and m_L as described in a later section of this paper. These quantities can then be used with an equation of state to determine the ullage pressure P_{TG}. If the system is purely a self-pressurizing system, the equations simplify considerably as can be seen by setting $\dot{m}_{PG} = 0$ and noting that the properties subscripted with "*TG*" become "*VL*" throughout.

Note that $\dot{Q}_{VLC}$, which is the heat added to the vapor are a result of condensation, does not explicitly appear in the energy equation for the bulk liquid. Likewise, the heat extracted from the liquid resulting in evaporation $\dot{Q}_{VLB}$ does not explicitly appear in the energy equation for the ullage vapor. The reason is that these quantities are the heat required for phase change and this heat is not transferred across the control volume boundaries rather the heat associated with phase change appears in the energy equation as a product of enthalpy and mass flow rate (e.g. $\dot{m}_{VLB} h_{VLB}$ and $\dot{m}_{VLC} h_{LC}$ terms).

The tank wall temperature for the portions of the tank adjacent to the ullage gas and the bulk liquid is determined by solving two addition energy equations involving $\dot{Q}_{AWG}$ and $\dot{Q}_{AWL}$ respectively (described in the Auxiliary Equations section of this paper).

Model Implementation

The equations that form the mathematical model are first order in time. It is quite straightforward to create a single subroutine that computes changes in the dependent variables over a time interval. The tank geometry,

Downloaded by STANFORD UNIVERSITY on April 12, 2022 | http://arc.aiaa.org | DOI: 10.2514/6.2005-3549

ambient conditions and a feed-system discharge coefficient are specified along with the initial propellant mass, propellant temperature and chamber pressure. The heat and mass transfer terms and thermodynamic properties (described in the next two sections) are evaluated at each time step. In the current implementation, a fourth order Runge-Kutta algorithm with a time step of 0.001 sec was used. The end results are predicted time histories of the ullage gas-vapor mixture and the bulk liquid pressure and temperature along with several other quantities of interest. The following equations and constraints supplement those already described.

It was pointed out earlier that when a liquid and vapor are not in phase equilibrium, the surface temperature T_S is not equal to the saturation temperature T_{SAT}. However, the T_S deviations from T_{SAT} are probably small, so in the current model:

$$T_S = T_{SAT} \tag{22}$$

Setting the surface temperature equal to the saturation temperature constrains the solution to what may be termed quasi-phase equilibrium but because the tank is not in thermal equilibrium, the ullage gas and bulk liquid can be at temperatures other than the saturation temperature. Furthermore, in a strict sense, phase equilibrium is not possible in an open system with one outlet. This condition can be easily modified upon the development of a more rigorous liquid-vapor interfacial theory. Using mass conservation, the liquid and gas volume rate-of-change are:

$$\dot{V}_L = (- \dot{m}_{PROP} - \dot{m}_{VLB} + \dot{m}_{VLC} - V_L \dot{r}_L) / r_L \tag{23}$$

$$\dot{V}_{TG} = -\dot{V}_L \tag{24}$$

If all of the liquid is exhausted from the tank then $\dot{V}_{TG} = \dot{V}_L = 0$ while vapor is being expelled from the tank.

The mass of the tank gas can be determined from:

$$\dot{m}_{TG} = \dot{m}_{PG} + \dot{m}_{VLB} - \dot{m}_{VLC} \tag{25}$$

$$\dot{m}_{VL} = \dot{m}_{VLB} - \dot{m}_{VLC} \tag{26}$$

$$m_{TG} = m_{VL} + m_{PG} \tag{27}$$

And for the vapor-only portion of the flow (i.e. after all liquid is exhausted from the tank):

$$\dot{m}_{TG} = \dot{m}_{PG} - \dot{m}_{PROP} \tag{28}$$

State Equation

The vapor of many commonly used propellants behave as a van der Waals gas (i.e. not as an ideal gas, $Z \approx 0.54$ for saturated N_2O at room temperature) hence, the Peng-Robinson equation of state[8] is used to determine the pressure of the tank gas (here, $R_m = 8.3144$ J/mol K):

Downloaded by STANFORD UNIVERSITY on April 12, 2022 | http://arc.aiaa.org | DOI: 10.2514/6.2005-3549

$$P_{TG} = \frac{R_m T_{TG}}{v_{TG} - b} - \frac{a}{{v_{TG}}^2 + 2bv_{TG} - b^2} \quad \text{(kPa)} \qquad (29)$$

where: $v_{TG} = M_{TG} V_{TG} / m_{TG}$ and P_{TG} is in kPa.

$$a = a_c a \ , \quad a_c = \frac{0.45724 {R_m}^2 {T_c}^2}{P_c} \ , \quad b = \frac{0.07780 R_m T_c}{P_c} \qquad (30)$$

and

$$k = 0.37464 + 1.54226w - 0.26992w^2 \qquad (31)$$

$$a = \left[1 + k\left(1 - \sqrt{\frac{T_{TG}}{T_c}}\right)\right]^2 \qquad (32)$$

Note that if an inert pressurant gas is introduced, mixing rules should be applied to the equation of state. For N_2O, T_c=309.56 ^oK, P_c=7.238×10^6 pa, and w=0.160.

Auxiliary Equations

The model assumes that the temperature in the vessel wall adjacent to the liquid is different from that adjacent to the ullage gas because the convective heat transfer rates contained in $\dot{Q}_{LW}$ and $\dot{Q}_{GW}$ are disparate. A conservation of energy analysis of the vessel walls leads to:

$$\dot{T}_{WL} = (\dot{Q}_{AWL} - \dot{Q}_{LW}) / (m_{WL} c_{P_{WL}}) \qquad (33)$$

$$\dot{T}_{WG} = \{ \dot{Q}_{AWG} + \dot{Q}_{GW} + c_{P_{WL}} (T_{WL} - T_{WG}) \dot{m}_{WG} \} / (m_{WG} c_{P_{WG}}) \qquad (34)$$

The mass flow rate $\dot{m}_{prop}$ through the propellant feed system is modeled using an aggregate discharge coefficient C_D and the following relations:

$$\dot{m}_{prop} = C_D A_{injector} Y \sqrt{2 r \Delta P} \quad \text{(for liquid and unchoked gas flow)} \qquad (35)$$

$$\dot{m}_{prop} = C_D A_{injector} Y \sqrt{2 r_{TG} P_{TG}} \quad \text{(for choked gas flow)} \qquad (36)$$

Where ΔP is the pressure difference between the propellant tank and the combustion chamber. The expansion factor Y is the ratio of the flow rate with compressibility to that without compressibility ($Y \cong 1$ when liquid is flowing through the system). The discharge coefficient is a geometry and Reynolds number dependent quantity that is the ratio of the actual flow rate to the ideal flow rate. The effects of cavitation (if present) on the propellant mass flow rate are taken into account through a reduction in the discharge coefficient.

Downloaded by STANFORD UNIVERSITY on April 12, 2022 | http://arc.aiaa.org | DOI: 10.2514/6.2005-3549

Downloaded by STANFORD UNIVERSITY on April 12, 2022 | http://arc.aiaa.org | DOI: 10.2514/6.2005-3549

Thermodynamic Properties

Several approaches can be taken to determine the thermodynamic properties required by the model. The techniques range from table lookups of measured quantities to the utilization of sophisticated equation-of-state based multi-component software programs. The choice should be made based on the number of propellant components, the number of phases involved, the anticipated data range required, the availability of data, accuracy and the degree of generality desired. It is generally believed that measured property data is more accurate than that derived from state equations. For example, the measured saturated liquid density is 8.9% higher than that predicted by the Peng Robinson state equation for N_2O at 299 ^oK. On the other hand, very few simplifications can be made, a priori, to reduce the quantity of measured data required to a manageable level. For instance, the compressibility factor Z for N_2O vapor typically ranges between 0.4 and 0.7 (while liquid is in the tank) and therefore, ideal gas approximations are not valid. In addition, phase non-equilibrium implies that the properties can deviate from saturation values and therefore are functions of at least two variables. These considerations have lead to the use of departure functions[9], derived from the Peng-Robinson equation of state, for enthalpy, internal energy and specific heat.

There are several advantages to using an equation of state to obtain fluid properties over other approaches. Foremost is that the method is applicable over wide ranges of temperature and pressure. It can be used for the representation of vapour-liquid, liquid-liquid and supercritical fluid phase equilibria. Secondly, the model will be consistent. Errors arising from intermingling data and equations from disparate sources will be avoided. Finally, one can change the fluid being investigated with minimal effort.

For the Peng-Robinson equation of state, the specific enthalpy and internal energy departure functions take the following form[10]:

$$h - h^{ig} = \frac{R_u T}{M}\left[(Z-1) - \ln\left(\frac{Z+2.414B}{Z-0.414B}\right)\frac{A}{2.828B}\left(1+\frac{k\sqrt{T_r}}{\sqrt{a}}\right)\right] \quad \text{(J/kg)} \qquad (37)$$

$$u - u^{ig} = \frac{R_u T}{M}\left[-\ln\left(\frac{Z+2.414B}{Z-0.414B}\right)\frac{A}{2.828B}\left(1+\frac{k\sqrt{T_r}}{\sqrt{a}}\right)\right] \quad \text{(J/kg)} \qquad (38)$$

Where $R_u = 8314.4$ J/(kmole K), $A = \frac{aP}{R_m{}^2 T^2}$, $B = \frac{bP}{R_m T}$ ($R_m = 8.3144$ J/mol K in the expressions for A and B) and $T_r = T/T_c$. The compressibility factor is computed as a root of the dimensionless form of the Peng-Robinson equation of state, as follows:

$$Z^3 - (1-B)Z^2 + (A - 3B^2 - 2B)Z - (AB - B^2 - B^3) = 0 \qquad (39)$$

The largest of the three roots is the vapor compressibility factor and the smallest is the liquid compressibility factor. The conservation equations require determination of $\frac{d(u-u^{ig})}{dt}$. Examination of the time varying $u - u^{ig}$ departure function shows that it is a function of r, P and T but $\frac{\partial(u-u^{ig})}{\partial P} = 0$. Therefore by the expansion rule:

$$\frac{d(u-u^{ig})}{dt} = \frac{\partial(u-u^{ig})}{\partial T}\dot{T} + \frac{\partial(u-u^{ig})}{\partial r}\dot{r} = F_1\dot{T} + F_2\dot{r} \tag{40}$$

where:

$$F_1 = \frac{R_u T}{M}\left[\ln\left(\frac{Z+2.414B}{Z-0.414B}\right)\frac{A}{5.657B}\frac{k}{T_c a}\left(\sqrt{\frac{a}{T_r}}+k\right)\right] \quad \text{(J/kg K)} \tag{41}$$

$$F_2 = \frac{R_u T}{M}\left[-\left(\frac{Z}{r}\right)\frac{A}{Z^2+2BZ-B^2}\left(1+k\sqrt{\frac{T_r}{a}}\right)\right] \quad (\text{Jm}^3/\text{kg}^2) \tag{42}$$

When calculating F_2, care should be taken not to confuse the molar density r_m, calculated directly using the Peng Robinson equation of state, with r (i.e. $r_m = 10^3 r / M$, mole/m^3 where r has units of kg/m^3). The departure functions and these terms represent the real fluid effects on the model. For the limiting case of an ideal fluid, F_1 and F_2 approach 0, as expected.

Some of the thermodynamic properties, required by the model, are expressed in terms of standard thermodynamic functions[9]. The coefficients of these functions were determined by applying a nonlinear regression routine to data obtained from references 10 through 13.

$$\mu = AT^B/(1+C/T+D/T^2) \tag{43}$$

$$r = M(A/B^{1+(1-T/C)^D}) \tag{44}$$

$$ß = (-D/C)\ \ln(B)\ (1-T/C)^{D-1} \tag{45}$$

$$T_{SAT} = B/[A-\log_{10}(P/100000)]-C \tag{46}$$

$$P_{SAT} = 100000(10^{[A-(B/(T+C))]}) \tag{47}$$

$$\mu = A+BT+CT^2 \tag{48}$$

$$k = A+BT \tag{49}$$

$$\tilde{T} = T/1000 \tag{50}$$

$$c_P = 1000[A+B\tilde{T}+C\tilde{T}^2+D\tilde{T}^3+E/\tilde{T}^2]/M \tag{51}$$

$$h = 1000[A\tilde{T}+B\tilde{T}^2/2+C\tilde{T}^3/3+D\tilde{T}^4/4-E/\tilde{T}+F-H\ ]/M \tag{52}$$

Downloaded by STANFORD UNIVERSITY on April 12, 2022 | http://arc.aiaa.org | DOI: 10.2514/6.2005-3549

$$h = [A(1-T_r)^{(B+CT_r+DT_r^2+ET_r^3)}]/M \quad (53)$$

Table 2. Selected thermodynamic properties of N_2O.

N_2O				
Symbol	Phase	Units	Eq	Coefficients
m	Gas	kg/m sec	43	A=2.1150×10^{-6}, B=0.46420, C=305.70, D= 0.0 T_{min}=182 K, T_{max}=1000 K
r †	Liq*	kg/m^3	44	A=2.781, B= 0.27244, C= 309.57, D= 0.2882 T_{min}=160 K, T_{max}=310 K
ß	Liq	1/ K	45	A=2.781, B= 0.27244, C= 309.57, D= 0.2882 T_{min}=160 K, T_{max}=310 K
T_{SAT}	Gas*	K	46	A=4.80716087, B= 967.819748, C= 19.6368887 T_{min}=140 K, T_{max}=310 K
P_{SAT}	Gas*	pa	47	A=4.80716087, B= 967.819748, C= 19.6368887 T_{min}=140 K, T_{max}=310 K
m	Liq	kg/m sec	48	A=0.001877085, B= 1.1864×10^{-5}, C= 1.928×10^{-8} T_{min}=230 K, T_{max}=300 K
k	Liq	W/m K	49	A=0.39815, B= -0.0011510 T_{min}=182 K, T_{max}=310 K
k	Gas	W/m K	49	A=-0.007037, B= 0.0000823 T_{min}=190 K, T_{max}=430 K
c_P	Gas*	J/kg K	51	A=-5956.82087,B= 59029.4538, C= *-215342.983*, *D=276450.549*, *E=23.5743297* T_{min}=150 K, T_{max}=310 K
c_P^{ig}	Gas	J/kg K	51	A=21.62,B=72.81, C= *-57.78*, *D=18.3*, *E=0.0* T_{min}=150 K, T_{max}=310 K
c_P	Liq*	J/kg K	51	A=-131.55551, B= 3013.03128, C=-14290.1471, D=22239.8432, E=0.0 T_{min}=183 K, T_{max}=390 K
h_{lv}	Liq*	J/kg	53	A=2.686×10^7, B= 0.182, C=0.9387, D=-0.706, E= 0.0 T_{min}=182 K, T_{max}=310 K $T_{crit} = 309.6$ K
* Saturated liquid or vapor † For reference only (not used in the model)				

Table 3. Selected thermodynamic properties of Air.

Air				
Symbol	Phase	Units	Eq	Coefficients
m	Gas	kg/m sec	43	A=1.458×10^{-6}, *B=0.5*, C= 110.4, D= 0.0 T_{min}=100 K, T_{max}=400 K
k	Gas	W/m K	49	A=0.00715403, B= 0.00006085 T_{min}=100 K, T_{max}=2500 K
c_P	Gas	J/kg K	51	A=26.84107, B= 7.7816776, C= -1.8103208, D=0.14594026 E=-0.01102637 T_{min}=150 K, T_{max}=6000 K

Downloaded by STANFORD UNIVERSITY on April 12, 2022 | http://arc.aiaa.org | DOI: 10.2514/6.2005-3549

Downloaded by STANFORD UNIVERSITY on April 12, 2022 | http://arc.aiaa.org | DOI: 10.2514/6.2005-3549

Heat Transfer

Heat transfer is modeled between the regions within the tank and to the exterior of the tank using the concept of gas surface films, liquid surface layers and standard forced or free convection Prandtl-Grashof product approaches.[1,7]

The heat transfer models are summarized below. It turns out that for the ground-based blow-down test only two heat transfer processes are of significance. The first is associated with the evaporation of liquid. When liquid is vaporized, the heat required for vaporization is taken from the liquid thus reducing the temperature of the liquid. The second most significant heat transfer process is the transfer of heat from the ullage wall to the ullage vapor. All other heat transfer mechanisms have a negligible influence on the ullage pressure for the ground tests studied. These conclusions were determined by setting the heat transfer rates to zero in the model and observing the impact on the ullage pressure.

As will be shown below, the other heat transfer mechanisms modeled can be significant in flight or during filling and the ensuing warm-up process. Natural convection of the liquid and vapor in the tank is dependent on vehicle acceleration. In addition, there can be significant forced convection between the tank and the ambient environment.

Free convection is the heat transfer mechanism that is dominant in the tank interior. The heat transfer rate is determined from $\dot{Q} = hA\Delta T$. The average heat transfer coefficient $h = C\frac{k_f}{L_S}X^n$ is modeled based on empirical Nusselt number correlations of the type $Nu = C(Gr\,\mathrm{Pr})^n = CX^n$. For heat transfer modeling of forced convection to the ambient atmosphere (i.e. in flight), the Nusselt number is a function of a friction factor, *f* and Reynolds number. For further details and for the specific geometry and Nusselt number dependent coefficients (*C* and *n* exponent), see Refs. 1 and 7.

The characteristic length L_S and the area A, specified in the equations shown below, are for a cylindrical tank. Heat transfer from the tank end caps has been neglected because they are of smaller area. Other geometries can be implemented by replacing the geometry specific quantities in the following expressions with those that are appropriate as given in many heat transfer books (e.g. see reference 7). The thermodynamic properties used in the following equations are evaluated at the temperature of the relevant media (as indicated by the subscript) unless otherwise noted.

The free convection heat transfer between liquid and wall adjacent to liquid ($L_{LW} = z$, $A_{LW} = pDz$) is:

$$X_{LW} = (L_{LW}{}^3 r_L{}^2 a ß_L \left|T_L - T_{WL}\right| / \mu_L{}^2)\,(c_{P_L}\,\mu_L / k_L) \tag{54}$$

$$h_{LW} = C_{LW} k_L X_{LW}{}^{n_{LW}} / L_{LW} \tag{55}$$

$$\dot{Q}_{LW} = h_{LW} A_{LW} (T_{WL} - T_L) \tag{56}$$

The free convection heat transfer between liquid and liquid surface layer ($L_{LS} = D$, $A_{LS} = pD^2/4$) is:

$$X_{LS} = (L_{LS}{}^3 r_L{}^2 a ß_L \left|T_L - T_S\right| / \mu_L{}^2)(c_{P_L}\,\mu_L / k_L) \tag{57}$$

$$h_{LS} = C_{LS} k_L X_{LS}{}^{n_{LS}} / L_{LS} \tag{58}$$

$$\dot{Q}_{LS} = h_{LS} A_{LS}(T_L - T_S) \tag{59}$$

Heat transfer between gas and liquid surface layer ($L_{GS} = D$, $A_{GS} = pD^2/4$) is:

$$X_{GS} = (L_{GS}{}^3 r_{TG}{}^2 a ß_{GSF} |T_{TG} - T_S| / \mu_{GSF}{}^2)(c_{P_{GSF}} \mu_{GSF} / k_{GSF}) \tag{60}$$

$$h_{GS} = C_{GS} k_{GSF} X_{GS}{}^{n_{GS}} / L_{GS} \tag{61}$$

$$\dot{Q}_{GS} = h_{GS} A_{GS}(T_S - T_{TG}) \tag{62}$$

In the ullage, it is assumed that there is an appreciable difference between the wall and free-stream conditions. So, as is standard practice, the concept of a vapor film is applied and the temperature used to evaluate the properties used to compute the heat transfer between the wall and the vapor mixture is:

$$T_{GWF} = (T_{TG} + T_{WG})/2 \tag{63}$$

Heat transfer from the ullage wall to the gas ($L_{GW} = z_{\max} - z$, $A_{GW} = pD(z_{\max} - z)$) is:

$$X_{GW} = (L_{GW}{}^3 r_{TG}{}^2 a ß_{GWF} |T_{TG} - T_{WG}| / \mu_{GWF}{}^2)(c_{P_{GWF}} \mu_{GWF} / k_{GWF}) \tag{64}$$

$$h_{GW} = C_{GW} k_{GWF} X_{GW}{}^{n_{GW}} / L_{GW} \tag{65}$$

$$\dot{Q}_{GW} = h_{GW} A_{GW}(T_{TG} - T_{WG}) \tag{66}$$

During the period of time when liquid is being expelled from the tank, vaporization takes place at the liquid-vapor mixture interface or possibly within the bulk liquid in the form of boiling. The heat required to produce the phase change is taken from the liquid and is expressed as:

$$\dot{Q}_{VLB} = \dot{m}_{VLB} h_{lv} \tag{67}$$

Where h_{lv} is the latent heat of vaporization. Condensation can occur resulting in heat transferred back to the liquid:

$$\dot{Q}_{VLC} = \dot{m}_{VLC} h_{lv} \tag{68}$$

For ground tests with no cross wind, the heat transfer mechanism between the tank and external environment is free convection ($L_{SA} = z_{\max}$):

Downloaded by STANFORD UNIVERSITY on April 12, 2022 | http://arc.aiaa.org | DOI: 10.2514/6.2005-3549

$$X_{SA} = (L_{SA}{}^3 r_A{}^2 a ß_A |T_{AS} - T_{WL}| / \mu_A{}^2)(c_{P_A} \mu_A / k_A) \tag{69}$$

$$h_{SA} = C_{SA} k_A X_{SA}{}^{n_{SA}} / L_{SA} \tag{70}$$

During ground tests with a non-zero cross wind, the forced convection heat transfer coefficient is:

$$h_A = C_A k_A R_e{}^{n_A} / D \tag{71}$$

During flight, forced convection heat transfer can be quite substantial because a high flight Mach number can result in a high recovery temperature[7]. The forced convection heat transfer coefficient is:

$$f = 0.0592 R_e{}^{-0.2} \tag{72}$$

$$h_A = 0.5 C_A f r_{AF} c_{P_{AF}} V_A \tag{73}$$

The heat transfer from the tank wall to the external environment for the portion of the tank containing liquid and also for the portion containing vapor mixture is ($A_{AWL} = pDz$, $A_{AWG} = pD(z_{\max} - z)$):

$$\dot{Q}_{AWL} = h_A A_{AWL} (T_{AR} - T_{WL}) \tag{74}$$

$$\dot{Q}_{AWG} = h_A A_{AWG} (T_{AR} - T_{WG}) \tag{75}$$

Mass Transfer

Mass can be injected into the ullage in the form of an inert pressurant gas. Liquid followed by a vapor flow (for self-pressurizing systems) or a gas-vapor mixture (for pressure-fed systems) flows out of the tank. Mass can be transported from the liquid to the ullage through evaporation or boiling and mass can be transported to the liquid through condensation. All of these transport phenomena are modeled. In the context of this model, "boiling" refers to a phase change of the bulk liquid to a vapor. Differentiation between the various mechanisms, (i.e. pool boiling, film boiling, evaporation…etc.) resulting in the phase, is not required by the model.

For self-pressurizing propellant systems, the mass transfer rate of liquid to vapor must be properly modeled to obtain a reasonable ullage pressure prediction. Physically, the evaporation process involves convection, diffusion and is non-stationary (i.e. the liquid surface is regressing with time). Unfortunately, there is no simple way to model this evaporative process from first principles. Concepts from "high mass transfer rate theory" and other theories are invoked, as shown in Appendix A, in the development of the following semi-empirical expression:

$$\dot{m}_{VLB} = h_{LSB} (A_{LS} / h_{lv}) (T_L - T_{SAT}) \tag{76}$$

Where h_{LSB} is the heat transfer coefficient associated with the liquid to vapor phase change.

Downloaded by STANFORD UNIVERSITY on April 12, 2022 | http://arc.aiaa.org | DOI: 10.2514/6.2005-3549

In most cases, the liquid in the propellant tank will be stirred by heat-transfer initiated convection. It is believed that liquid stratification will only develop in the rare instances when the heat transfer between the vessel and the external environment is such that convection is not induced in the bulk liquid (i.e. isothermal).

The essence of the evaporation model is that the mass-transfer rate from the liquid to vapor is proportional to the difference between the liquid temperature and the vapor saturation temperature times a heat transfer coefficient h_{LSB} that is related to the transport of liquid (by convection) to the liquid surface.

In a single component self-pressurizing system the vapor in the ullage is saturated or nearly saturated and typically the ullage walls and bulk liquid are warmer than the ullage gas so condensation is unlikely. In a two component system, mass transfer by condensation can happen if the expansion reduces the tank gas temperature to the dew point of one of the constituents. At the dew point temperature, a cloud can form that in turn, releases the corresponding heat of condensation to the vapor phase. Condensation on the ullage walls can happen if the wall temperature reaches the dew point through some means. Under these circumstances, the mass transfer from the vapor to the liquid is:

$$\dot{m}_{VLC} = (P_{VL} - P_{VLC}) V_{TG} M_{VL} / (T_{TG} R_U \Delta t) \tag{77}$$

III. Model Validation

Several blow-down tests of the N_2O oxidizer delivery system, of a moderate size paraffin-fueled hybrid rocket, generated a reasonable dataset for comparison with this mathematical model (see Fig. 2). The test matrix was limited and additional validation is desirable. The case-specific data, required by the model, are presented in Table 4. The discharge coefficient, shown in Table 4, is that of the complete feed system (i.e. propellant tank exit to the combustion chamber) for the liquid flow portion of the test. In the current study, this quantity was determined post-test by matching the measured and modeled mass flow rates of the liquid at a point in time. The precise configuration of the feed line varied from test to test (thus, the variation in feed system discharge coefficient). For instance, in some of the tests, a ball valve was

Table 4. Test matrix.

Test	C_D†	m_{loaded} (kg)	T (K)
1	0.425	20.0	286.5
2	0.365	16.68	278.5
3	0.365	14.59	271.5
4	0.09	24.12	291.3
† For liquid-only portion of the flow			

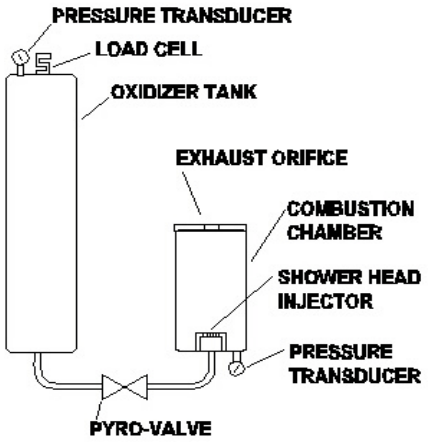

Figure 2. Blow-down test configuration.

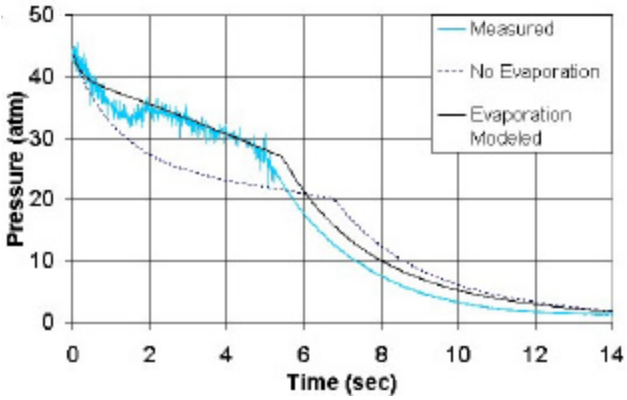

Figure 3. Comparison of measured and modeled ullage pressure for test 1.

Downloaded by STANFORD UNIVERSITY on April 12, 2022 | http://arc.aiaa.org | DOI: 10.2514/6.2005-3549

present in the feed line that was used to terminate the test prior to complete propellant consumption.

The fact that the magnitude of C_D is so low is indicative of flow-limiting cavitation occurring somewhere in the feed system. During the vapor-only portion, $C_D = 0.595$ was used as determined based on the geometry of the injector.

The capacity of the oxidizer tank is 0.0354 m^3. Typically, this tank was only partially filled in order to conserve N_2O (e.g. 64% full for test 1). The bulk liquid and gas temperatures are assumed to be equal to ambient prior to the start of the blow down. No temperature measurements were made within the tank.

The vertically oriented oxidizer tank was suspended from a load cell that measured the change of oxidizer mass during the test. Omega model PX303 pressure transducers were used to measure the ullage and combustion chamber pressure. The installed combustion chamber exhaust nozzle created a chamber pressure of 1.03 Mpa, nominal during the blow down. Data were acquired by a 12-bit analog-to-digital converter at a rate of 200 samples/sec per channel. The test was initiated under computer control by signaling a pyrotechnically actuated oxidizer valve (4 msec actuation period), inline between the oxidizer tank and combustion chamber, to open.

The most interesting test was the highest mass-flow rate test (referred to as test 1) and the modeling of this particular test is discussed in detail below followed by the results of three additional tests including one hot fire (test no. 4).

Shown in Fig. 3 is the measured ullage pressure history compared with the model for test 1. The measured pressure, during the liquid portion of the run, (between t=0 and approximately 5.2 secs) has a high frequency component superimposed on the generally decreasing trend in the data. At the 5.2 second point, the liquid in the tank is depleted and the remaining flow is vapor only.

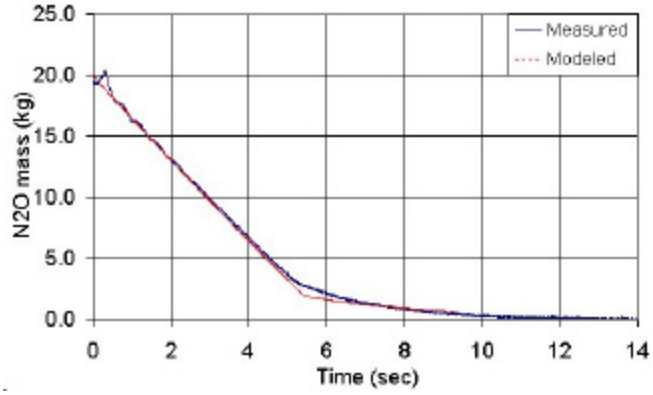

Figure 4. Comparison of measured and modeled propellant mass for test 1.

The measured pressure history shows that the transition from liquid to vapor flow is not as precisely defined as the model indicates. This is probably because in the transition from liquid to vapor flow, there is a period of time when the flow is a vapor and liquid mixture. Also shown in Fig. 3 is a modeled result wherein no heat transfer (thus no mass transfer, i.e. $\dot{m}_{VLB} = 0$) was permitted between the liquid and ullage gas. The difference between the two modeled results is indicative of the extent that propellant evaporation affects the ullage pressure and the importance of the evaporation model.

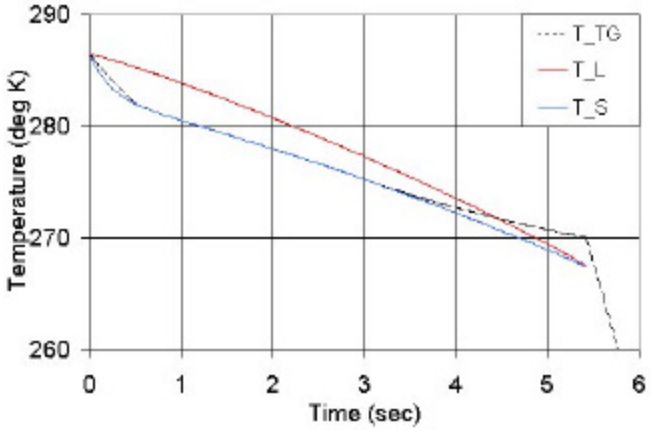

Figure 5. Modeled temperature time history for test 1.

An interesting phenomenon was observed in the measured ullage pressure time history for this high mass flow test that was not observed in other tests. At approximately 1.6 seconds after the oxidizer shutoff valve was opened, the pressure in the tank started to increase even though the mass flow rate out of the tank, as

Downloaded by STANFORD UNIVERSITY on April 12, 2022 | http://arc.aiaa.org | DOI: 10.2514/6.2005-3549

shown in Fig. 4, was constant.

The origin of this unexpected 2 atm ullage pressure variation is thought to be stratification that developed in the liquid. Unlike the other blow-down tests, a heat blanket was applied to the exterior of the oxidizer tank prior to test 1 in order to increase the liquid temperature and therefore the ullage pressure. It appears that the heating was not uniform. As the blow down commenced, cool liquid was churned up from the lower portion of the tank that temporarily suppressed the evaporation rate.

Presented in Fig. 4 is a comparison between the modeled and measured oxidizer tank mass time histories. A running average has been applied to the measured data to average out the high frequency inertial effects caused by vibration. Even so, at the start of the blow down, the measured trace shows some low frequency transient effects that are probably inertial in origin (for instance, the measured mass at *t=0.2* secs is higher than the initial mass). The comparison shows that the modeled and measured oxidizer mass flow rates, during the liquid and vapor flow phases, agree as well as can be expected. Furthermore, the specified feed system discharge coefficients properly models the mass discharge behavior of the system.

It should be noted that, like thrust measurements, obtaining an accurate measurement of the oxidizer mass time history is difficult. The load cell used for these measurements also registers inertial effects arising from vibration during the blow down and the component of thrust (if any) aligned with the axis of the load cell. In the current setup, the oxidizer tank was connected to the combustion chamber via a metal tube bent 90^o so that the thrust produced would be directed perpendicular to the axis of the load cell used to measure the oxidizer mass. The combustion chamber was not suspended by the load cell so the flexibility of the tube between the oxidizer tank and combustion chamber influenced the oxidizer mass measurement to a small degree.

The modeled bulk liquid, and ullage vapor temperature time histories along with the saturation temperature are presented in Fig. 5. The histories show that the temperature of the bulk liquid is up to 3.5^o K warmer than that of the ullage vapor. At transition point between liquid and vapor expulsion, the bulk liquid temperature is equal to the surface temperature as expected.

A few numerical experiments were performed to assess the importance of various terms in the conservation equations. The first series of tests involved individually turning off each heat transfer term and then observing the impact on the predicted results for test 1. It was found that only $\dot{Q}_{VLB}$ had a significant impact. When $\dot{Q}_{VLB}$ was set to zero, the predicted ullage pressure deviated from the baseline by up to 10.6 percent.

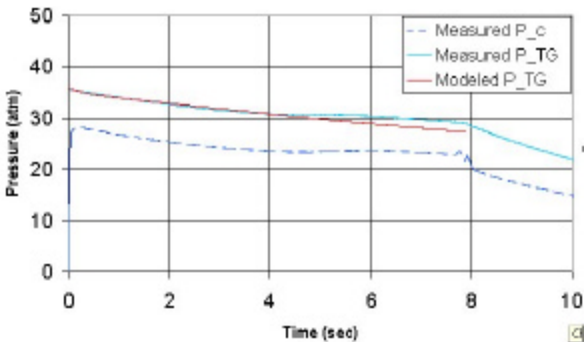

Figure 6. Comparison of measured and modeled pressure time histories for test 2.

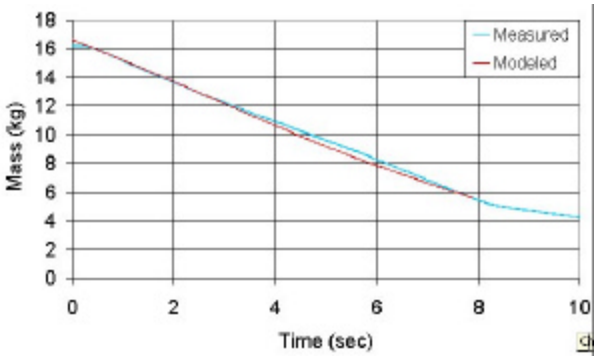

Figure 7. Comparison of measured and modeled propellant mass for test 2.

Downloaded by STANFORD UNIVERSITY on April 12, 2022 | http://arc.aiaa.org | DOI: 10.2514/6.2005-3549

The significance of the real-fluid effects were assessed by comparing the relative magnitude of F_{1_L} to ${c_{V_L}}^{ig}$ and also $F_{1_{TG}}$ to ${c_{V_{TG}}}^{ig}$. The quantity F_1 is equal to zero for an ideal fluid and $F_1 + {c_V}^{ig}$ is inversely proportional the rate of temperature change as expressed by the energy equation.. It was found that F_{1_L} was up to 37 percent of ${c_{V_L}}^{ig}$ and $F_{1_{TG}}$ was up to 6.5 percent of ${c_{V_{TG}}}^{ig}$ at the beginning of the blow down (when the propellant properties are closest to their critical point values). Therefore inclusion of real fluid effects is essential.

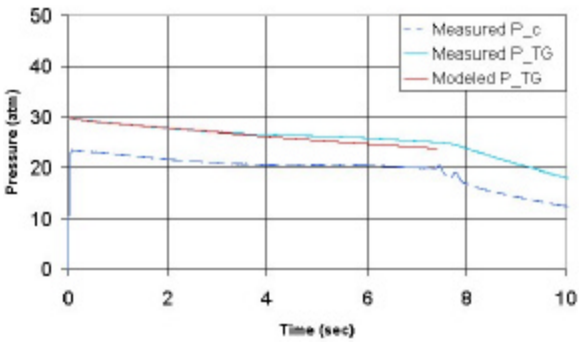

Figure 8. Comparison of measured and modeled pressure time histories for test 3.

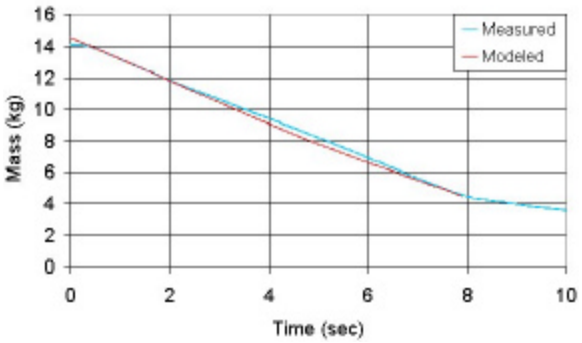

Figure 9. Comparison of measured and modeled propellant mass for test 3.

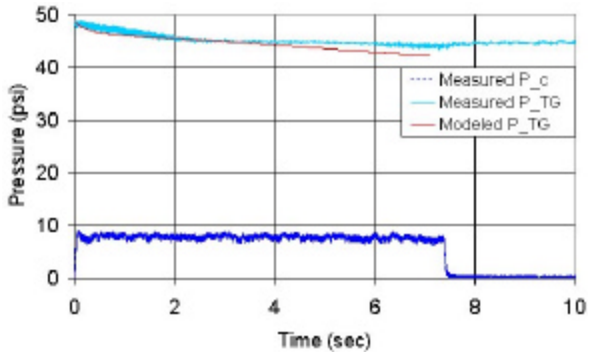

Figure 10. Comparison of measured and modeled pressure time histories for test 4.

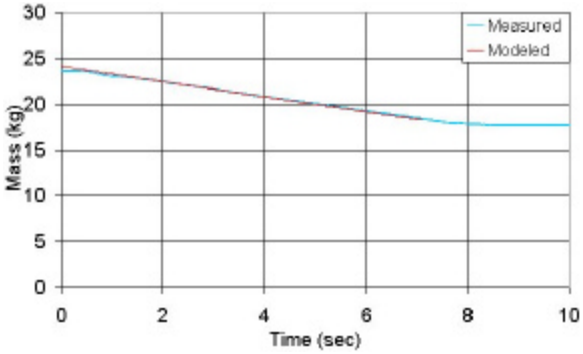

Figure 11. Comparison of measured and modeled propellant mass for test 4.

Shown in Figs 6-11 are comparisons of modeled and measured ullage pressure and oxidizer mass for tests 2-4. The measured combustion chamber pressure is also shown. Only the liquid portion of the flow was modeled because, unlike test 1, the oxidizer feed line valve was closed to terminate the liquid flow prior to the onset of vapor flow. The comparison between the measured and model results is good particularly during the early portion of the tests.

Presented in Fig. 12 is a comparison between the predicted oxidizer tank and chamber pressure for a modeled ground test and a modeled flight with an apogee of 22 km. As can be seen, the heat transfer to the ambient environment effect is rather small for this sounding rocket case. The minor difference is

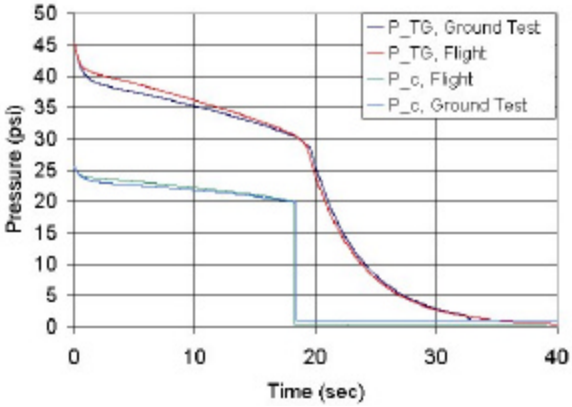

Figure 12. Comparison of modeled ground test and flight pressure time histories.

Downloaded by STANFORD UNIVERSITY on April 12, 2022 | http://arc.aiaa.org | DOI: 10.2514/6.2005-3549

attributed to the heat transfer from the wall adjacent to the ullage to the ambient environment during ascent (i.e. $\dot{Q}_{AWG}$). These effects have been retained in the model because they could be of greater significance for rockets with long burn times.

IV. Conclusions

A thermodynamic model of a propellant tank pressurization system has been developed and used to model the self-pressurizing oxidizer system of a moderate size hybrid rocket. The model does not assume thermo or phase equilibrium (although the liquid surface is set equal to the saturated vapor temperature) and is applicable to propellants that exhibit real-fluid behavior.

During the development of the model, it was determined that the rate of propellant vaporization has, far and away, the greatest impact on the accurate prediction of ullage pressure for the highly volatile nitrous oxide propellant studied. To this end, a new model of the propellant evaporation mass transfer rate ($\dot{m}_{VLB}$) was developed. The evaporation model required a factor to compensate for inadequacies in the heat transfer coefficient associated with the phase change from liquid to vapor. Additional experiments specifically designed to measure heat transfer could reduce the level of empiricism employed in the model.

It is believed that an unexpected variation in ullage pressure, during blow-down test 1, was caused by an instability of stratified liquid in the tank. The instability resulted in the transport of cool liquid to the surface that initially suppressed the evaporation process.

For nitrous oxide, the real fluid effects are significant. Propellant tank modeling, wherein the ullage gas is assumed to behave as an ideal gas, is woefully inadequate. The use of advanced equations of state and departure functions readily enables inclusion of real-fluid effects at the cost of a small reduction in accuracy for conditions close to the propellant critical point.

The heat transfer rate between the propellant vapor and the ullage tank wall $\dot{Q}_{GW}$ was found to have a minor impact on the ullage pressure for the ground-based blow-down tests modeled. For short duration ground based tests, all of the heat transfer terms are negligible with the exception of $\dot{Q}_{VLB}$ which has a major impact. In flight, the importance of the heat transfer terms should be evaluated on a case-by-case basis.

The modeled and measured ullage pressure and oxidizer mass-flow rate were found to be in reasonably good agreement for the four tests considered.

Appendix A

As pointed out in the main text, accurately determining the liquid-to-vapor mass flux is crucial to the prediction of propellant tank pressurization. Since there is a net mass flux from the liquid to the vapor, the phases are not in equilibrium and therefore the temperature of the liquid-vapor interface cannot be equal to the saturation temperature. The obvious question that follows is what is the interfacial temperature? Efforts to reconcile various non-equilibrium evaporation theories (employing Kinetic Theory[14] and Statistical Rate Theory[15]) with interfacial temperature measurements have been largely unsuccessful.[16] Typically, the theories under predict temperature jumps across the liquid-vapor interface by factors of 10 to 30. Hence, they under predict the mass

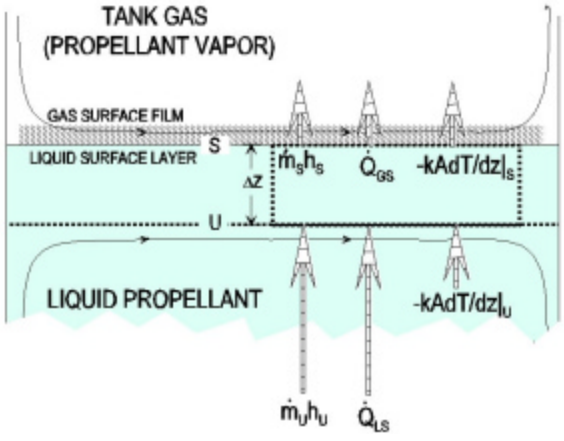

Figure 13. Schematic showing the liquid surface layer energy balance.

Downloaded by STANFORD UNIVERSITY on April 12, 2022 | http://arc.aiaa.org | DOI: 10.2514/6.2005-3549

flux from liquid to vapor because heat and mass fluxes are inextricably related.

The approach taken here to model the interfacial region between the liquid, is to establish a surface liquid layer of varying temperature. It is assumed that the effects of phase non-equilibrium on the interfacial temperature are small and therefore, the temperature at the vapor-liquid interface is the saturated vapor temperature. Heat and mass are transported across the layer as shown in Fig. 13. Hence, the ullage pressure is dependent on the rate of mass transfer from the liquid to the vapor.

The basic configuration is that of a receding liquid surface layer with convection-induced flow within the bulk liquid and gas (Note: *h* refers to enthalpy in this figure). In the final analysis, the liquid layer is non-stationary, it is insufficient to simply consider the effects of molecular diffusion. The concepts of high-mass-flow rate theory[17] are relevant. In this theory, the heat transfer from the liquid to the vapor is accelerated by an additional convection current induced by the mass transfer process itself (commonly referred to as a blowing effect in high-mass-flow rate theory). In the following analysis, the blowing effect is included in a simplistic manner as a contributor to an empirical factor that modifies the mass flow rate.

The energy equation can be written for the control volume shown in Fig. 13 as follows:

$$\dot{Q}_{LS} + \dot{m}_U h_U - kA\frac{dT}{dz}\Big|_U = \dot{Q}_{GS} + \dot{m}_S h_S - kA\frac{dT}{dz}\Big|_S \tag{A1}$$

Recognizing that under steady state conditions, $\dot{m}_U = \dot{m}_S$ and also that the enthalpy change is equal to the latent heat of vaporization (i.e. $h_S - h_U = h_{lv}$) and assuming that the heat transfer by conduction is small then:

$$\dot{m}_{VLB} = \frac{\dot{Q}_{LS} - \dot{Q}_{GS}}{h_{lv}} \tag{A2}$$

$$\dot{m}_{VLB} = \frac{h_{LS} A_{LS} (T_L - T_S) - h_{GS} A_{GS} (T_S - T_{TG})}{h_{lv}} \tag{A3}$$

This is the governing equation that should be solved to determine the mass transfer $\dot{m}_{VLB}$ rate from the liquid to vapor. The chief difficulty is that the heat transfer coefficients h_{GS} and h_{LS} used in determining $\dot{Q}_{GS}$ and $\dot{Q}_{LS}$ are not easily obtained (particularly if the liquid is stratified). One additional simplification can be made and that is to ignore the effect of $\dot{Q}_{LS}$ on $\dot{m}_{VLB}$ because for the cases studied here, $\dot{Q}_{GS} << \dot{Q}_{LS}$. This is tantamount to saying that the evaporation is driven by the heat transfer from the bulk liquid to the surface.

If the model is restricted to one component and the surface temperature is assumed to equal the saturation temperature, then:

$$\dot{m}_{VLB} = h_{LSB}(A_{LS}/h_{lv})(T_L - T_{SAT}) \tag{A4}$$

In the above expression, $h_{LSB} = Eh_{LS}$ where E is an empirical factor (for N_2O, $E = 2.1\times10^4$). It should be noted that the values for E are dependent on the oxidizer used. In the current study, these values were determined by trial and error comparisons of modeled and measured ullage pressure time histories for N_2O.

Downloaded by STANFORD UNIVERSITY on April 12, 2022 | http://arc.aiaa.org | DOI: 10.2514/6.2005-3549

The most objectionable aspect of this model is the large magnitude of the empirical factor E. The fact that the model predicts the correct evaporation rate over a wide range, (mass flux rates ranging between 0 and 18 kg/m^2 sec for the cases shown) as demonstrated by the close match between the measured and modeled ullage pressure and propellant mass histories, is evidence that the functional form of the model is reasonable. It is likely that E compensates for a heat transfer coefficient h_{LS} that is too low. The heat transfer coefficient was determined based on the assumption of turbulent natural convection within the liquid. Not included in h_{LS} are the effects of the liquid withdrawal from the tank, boiling (if present) or the effects of blowing, each of which should increase h_{LS}. This reinforces the need for experiments specifically designed to measure the data required to determine h_{LSB}.

An interesting inference from the form of this evaporation model is that stirring the bulk liquid propellant may result in a higher evaporation rate (by effectively increasing the heat transfer coefficient h_{LS}). This would be beneficial in several respects. The liquid would not become stratified in the tank. The ullage pressure reduction, that occurs as propellant is expelled from the tank, would be less resulting in increased rocket performance. Finally, the whole propellant pressurization and expulsion process would be more repeatable.

Downloaded by STANFORD UNIVERSITY on April 12, 2022 | http://arc.aiaa.org | DOI: 10.2514/6.2005-3549

Acknowledgment

We'd like to acknowledge the Stanford University Office of Technology Licensing and also NASA cooperative agreements NAG3-2615 with the NASA Glenn Research Center and agreements NCC2-1172 and NCC2-1300 with the NASA Ames Research Center.

References

1. Ring, Elliot ed., *Rocket Propellant and Pressurization Systems*, Prentice-Hall Inc., Englewood Cliffs, NJ, 1964 (unfortunately, out of print).

2. Pasley, G. F., "Optimization of Stored Pressurant Supply for Liquid Propulsion Systems," J. of Spacecraft, Vol 7, No. 12. 1970, p. 1478-1480.

3. Holt, K., Majumdar, A., Steadman, T. and Hedayat, A., "Numerical Modeling and Test Data Comparison of Propulsion Test Article Helium Pressurization System," AIAA 2000-3719, Huntsville, Al.

4. Majumdar, A. and Steadman, T., "Numerical modeling of Pressurization of a Propellant Tank," J. of Propulsion and Power, Vol 17, No. 2, 2001, p. 385-390.

5. Panzarella, C. H. and Kassemi, M., "On the Validity of Purely Thermodynamic Descriptions of Two-Phase Cryogenic Fluid Storage," J. of Fluid Mech. (2003), Vol 484, pp. 41-68.

6. Giordano, D. and De Serio, M. "A Thermodynamic Model of Hydrazine that Accounts for Liquid-Vapor Phase Change," AIAA A01-31429, 35th Thermophysics Conference, Anaheim, Ca. 2001.

7. Holman, J.P., *Heat Transfer*, McGraw-Hill Inc., New York, NY, 1976.

8. D. Y. Peng and D. B. Robinson, "A New Two-Constant Equation of State," *Ind. Eng. Chem. Fundam.* Vol. 15, No. 1, p. 59-64. (1976).

9. Reid, R.C., Prausnitz, J.M. and Sherwood, T.K. *The Properties of Gases and Liquids*, 3rd ed., McGraw-Hill, New York, NY 1977.

10. Ho, C. Y. Ed., "Properties of Inorganic and Organic Fluids" CINDAS Data Series, Vol V-1, Hemisphere Inc, NY, 1988.

11. Elliot, J. R. and Lira, C.T., *Introductory Chemical Engineering Thermodynamics*, 6th ed., Prentice Hall, 1999.

12. Matheson Gas Data Book, 7th Ed. McGraw-Hill, Parsippany, NJ, 2001.

13. NIST Chemistry Webbook. http://webbook.nist.gov/chemistry/ .

14. Schrage, R.W., "A Theoretical Study of Interphase Mass Transfer," Columbia University Press, 1953.

15. Ward, C.A. and Fang, G., "Expression for Predicting Liquid Evaporation: Statistical Rate Theory Approach," *Phys. Rev. E*, Vol 59, No. 1, 1999, p. 429-440.

16. Kumar, V. Danov, K.D. and Durst, F., "Extended Statistical Rate Theory for Liquid Evaporation," KONWIHR-QUARTL, 06-2003.

17. Mills, Anthony F. *Mass Transfer*, 2nd ed. Prentice Hall, Upper Saddle River, NJ. 2001.

Downloaded by STANFORD UNIVERSITY on April 12, 2022 | http://arc.aiaa.org | DOI: 10.2514/6.2005-3549